

Title	Multiple-simultaneous phased-array-antenna beam generation using an acousto-optic system
Authors	Riza, Nabeel A.
Publication date	1993-02-26
Original Citation	Riza, N. A. (1993) 'Multiple-simultaneous phased array antenna beam generation using an acousto-optic system', Proceedings of SPIE, 1790, Analog Photonics, Fibers '92, 1992, Boston, MA, United States, 26 February. doi: 10.1117/12.141722
Type of publication	Conference item
Link to publisher's version	10.1117/12.141722
Rights	© 1993 Society of Photo-Optical Instrumentation Engineers (SPIE). One print or electronic copy may be made for personal use only. Systematic reproduction and distribution, duplication of any material in this paper for a fee or for commercial purposes, or modification of the content of the paper are prohibited.
Download date	2023-12-09 21:46:48
Item downloaded from	https://hdl.handle.net/10468/10135

PROCEEDINGS OF SPIE

[SPIDigitalLibrary.org/conference-proceedings-of-spie](https://spiedigitallibrary.org/conference-proceedings-of-spie)

Multiple-simultaneous phased-array-antenna beam generation using an acousto-optic system

Riza, Nabeel

Nabeel A. Riza, "Multiple-simultaneous phased-array-antenna beam generation using an acousto-optic system," Proc. SPIE 1790, Analog Photonics, (26 February 1993); doi: 10.1117/12.141722

SPIE.

Event: Fibers '92, 1992, Boston, MA, United States

Multiple-simultaneous phased array antenna beam generation using an acousto-optic system

Nabeel A. Riza
General Electric Corporate Research & Development Center
P. O. Box 8, KWB617
Schenectady, N.Y 12301

ABSTRACT

An acousto-optic phased array antenna beamformer with N multiple simultaneous beam generation capability is proposed that has a wideband antenna operation feature. A version of the system is experimentally demonstrated using a single channel acousto-optic device driven by a signal of frequency f_c , and an acousto-optic device with N channels driven by signals with frequencies f_c+f_1, \dots, f_c+f_N , respectively. f_1, \dots, f_N control the carrier and phase values of the N independent beam generation signals, n being the beam number.

2. INTRODUCTION

Recently, we introduced and demonstrated an in-line additive acousto-optic (AO) architecture for controlling phase-based phased arrays [1-4]. This system provided the antenna drive signals for generating a single radar beam that can be rapidly scanned using one control signal. Multiple simultaneous phased array radar beams might be required for tracking multiple, fast moving targets. This paper describes a novel in-line additive acousto-optic (AO) architecture (see Fig.1) for generating the multi-band multiple signal sets for producing N multiple simultaneous beams. The basic architecture is an extension of the single beam generation AO design. Fundamental to the simultaneous, multiple beamforming operation is the use of a mutually incoherent, N -element laser-diode array, that allows the incoherent optical summation of the N different intensities at the output detector array, thus generating a linear summation of N independent, antenna beam control signals that are required to generate the desired N radar beams. The system uses two N -channel AO devices in cascade configuration, where the devices perform on a per channel basis, the dual function of generating the radar carrier by doppler shifting, and rf phase-shift generation via controlled diffracted beam deflections and interference. The corresponding channel pairs in the two N -channel AODs are fed by single sideband signals that individually control the carrier frequencies and phase shifts or beam positions of the N simultaneous beams.

An important consequence of this architecture is that several narrowband carriers with their appropriate phase shifts can be used to simulate wideband signal transmission and reception without large beam squint problems associated with frequency insensitive phase-based antenna control. This approach can enhance the range resolution of a typical phase-based radar without the use of time delays. One dimensional transmit/receive antenna beam scanning can be provided by this system, along with the simultaneous multifrequency capability.

A version of the acousto-optic phased array antenna beamformer (see Fig.2) with N multiple simultaneous beam generation capability is experimentally demonstrated using a single channel acousto-optic device (instead of a N -channel AOD) driven by a signal of frequency f_c , and an acousto-optic device with N channels driven by signals with frequencies f_c+f_1, \dots, f_c+f_N , respectively. f_1, \dots, f_N control the carrier and phase values of the N independent beam generation signals, n being the beam number. This work has also been described in ref. 5. Using $f_c=60$ MHz, and $N=2$, $0-2\pi$ phase control is achieved using $f_n=0-460$ KHz. A dynamic range of 54.5 dB@ 1 MHz and carrier-to-noise of 113.4 dB/Hz@ 1 MHz is measured for a 120 MHz carrier. When two N -channel AODs are used, single sideband signals are used to feed the devices.

3. THE EXPERIMENTAL CONCEPT PROCESSOR

Fig.2 shows a version of the multi-beam generation AO system. The N collimated beams from a N -element laser diode array are directed into a single channel AOD (called AOD1) using the cylindrical lens C1 with focal length FC1. AOD1 is driven by a signal of frequency f_c . Each Bragg matched beam incident on AOD1 generates its +1 order, positive doppler shifted beam, and its undiffracted (DC) beam. The N diffracted and DC order beam-pairs are collimated along the y direction using spherical lens S1 of focal length F1. Lenses C1 and S1 form an optical

system that preserves the spatial separation along the y direction between the N beam-pairs. A N-channel AOD (called AOD2) is placed in plane P1, such that the N spatially separated beam pairs are incident in the N independent channels of AOD2. Thus, each beam-pair interacts with its particular AOD2 channel. Cylinder C2 with a focal length FC2, and sphere S1, form a 1 : 1 imaging system along the x direction. This results in the DC beams from AOD1 being Bragg matched to the AOD2 channels, such that -1 order, negative doppler shifted beams are generated from the AOD2 channels. The +1 order beams from AOD1 pass through the AOD2 channels generating the +1 order diffracted beams that are collinear with the DC beams from AOD2; in addition, also generating a set of undiffracted DC beams (which are the +1 order beams from AOD1) that are almost collinear with their respective -1 order beams generated by AOD2 via the DC beams from AOD1. The AOD2 channels are driven by independently controlled signals, where, for instance, the nth channel is driven by a signal of frequency f_c+f_n , where f_n is the control frequency required to produce the nth radar beam at antenna beam scan angle q_n . Spheres S2 and S3 with focal lengths F2 and F3, respectively, form a 1 :M imaging system along the x direction, with $M=F3/F2$ being the optical magnification from plane P1 to plane P2. At plane P3, the front focal plane of lens S2, the unwanted N, DC light beams from AOD2 are blocked, thus allowing only the +1 and -1 beam pairs from AOD1 and AOD2, respectively, to interfere at plane P2. For optimum optical power system efficiency, the AODs should be operated at 50 % diffraction efficiencies. Spheres S2 and S3 also preserve the spatial separation along the y direction of the N, +1,-1 order beam pairs corresponding to the N mutually incoherent laser diodes. Cylinder C3 of focal length FC3 acts as an optical adder, combining the N light beam pairs, such that all beams appear as a line along the x direction where a fiber/photodiode array is placed for implementing the phase sampling and signal detection.

The signal from the mth photo-diode in the linear photo-diode array is a sum of the intensities resulting from the N, mutually incoherent beam pairs at the output plane P2. This photo-current is expressed as

$$i_m(t)=I_{m1}+I_{m2}+ \dots +I_{mn}+ \dots +I_{mN},$$

where the intensity I_{mn} consists of a constant bias term that forms the signal dc level, and an interferometric term that generates the nth-radar beam signal. This interferometric term is given by

$$\cos[2\pi(2f_c+f_n)t+\psi_n],$$

where ψ_n is the signal phase shift in radians required to position a beam at scan angle θ_n to broadside. Thus, $i_m(t)$ gives the required N signals needed to simultaneously generate N radar beams at scan angles $\theta_1, \theta_2, \dots, \theta_v, \dots, \theta_N$. Note, $\psi_n=(2\pi f_n)(l/M v)$, where l is the inter-fiber distance at plane P2 and v is the acoustic velocity in the AODs. Note that by varying f_n , the desired rf/microwave phase shift is generated by controlling the angular separation between the selected +1 and -1 order beams. Also note that the antenna carrier corresponding to the nth beam position is $2f_c+f_n$, implying that the antenna beams are frequency coded. For the system using two multichannel AODs with single sideband drive signals, the carrier frequency is independent of the control frequency f_n , and is given by $2f_c$.

4. EXPERIMENTAL RESULTS

For concept demonstration, a transmit-mode multi-beamforming optical system is tested at an rf of 120 MHz using flint glass AODs with $v=3.9$ mm/ μ sec, a 60 MHz center frequency, and a 10 μ sec time aperture. For receive-mode processing, the receive-signal set is electronically mixed with a replica of the transmit-mode signal set available from the optical processor [1-2]. The mixing operation combined with electronic low pass/intermediate frequency (IF) filtering generates in-phase baseband/IF signals that are added to maximize receiver output signal-to-noise ratio. A single channel flint glass AOD forms AOD1, while two single channel AODs are combined to form a N=2 channel AOD2. A 10 mW He-Ne laser, and a 5 mW He-Ne laser form the N=2 elements of a linear, mutually incoherent, laser array. The collimated beams from the two lasers are spatially separated along the y direction by appropriately positioning the lasers. AOD1 is fed by a $f_c=60$ MHz signal, while channel 1 and channel 2 in AOD2 are driven by rf signals with frequencies f_c+f_1 and f_c+f_2 , respectively. Here, all signals are phase-locked to a common 10 MHz stable clock. The focal lengths used for the lenses are: $FC1=15$ cm, $F1=15$ cm, $FC2=15$ cm, $F2=10$ cm, $F3=15$ cm, and $FC3=10$ cm. Two avalanche photodiodes (APDs) are placed at the output plane P2, with an inter-detector spacing of 12.7 mm. The outputs of the APDs drive 40 dB gain power amplifiers. All AOD channels are driven by 18 Vp-p @ 50 ohm rf signals. Fig.3 shows the spectrum analyzer output for a signal from one of the APDs, showing the presence of two simultaneous carriers, one at 120 MHz and the other at 123 MHz, used for generating two simultaneous radar beams. In this case, $f_1=0$ and $f_2=3$ MHz. The difference in the power levels for the two carriers relates to the different power levels and collimation optics for the two He-Ne lasers. The dynamic ranges measured for the 120 MHz and 123 MHz signals are 54.5 dB @ 1 MHz and 41.8 dB @ 1 MHz, respectively, as shown in

Fig.4. The carrier-to-noise ratio measured for the 120 MHz signal was 113.4 dB/Hz @ 1 MHz (see Fig.5). Carrier phase shift control is shown in Fig.6, where the two oscilloscope traces are outputs from the two APDs, with only channel 1 in AOD2 being driven, with channel 2 being off. In this way, only a 120 MHz + f_1 KHz carrier is observed, with phase shift control executed by changing f_1 (see Fig.7). Note that because the phase (or interference fringe) sampling process at the detector plane is periodic in nature, 2π phase shifts can be obtained over a periodic variation of the control frequency f_1 . In this experiment (see Fig.7), a change in f_1 (or f_2) of 460 KHz gives a phase shift of 2π radians. Thus, f_1 and f_2 can be independently set over a given frequency range to generate carrier signals with appropriately chosen frequencies and phase shifts to generate two radar beams in space. Fig.8 shows 0- 2π phase shift control for a 123.22 MHz + f_1 kHz carrier.

5. CONCLUSION

In conclusion, we have introduced an optical control system for high speed (200 ns) phased array antenna beam switching and scanning that can generate (both transmit and receive operation in one scan dimension) multiple simultaneous beams in space. The architecture can be used to simulate near squint free wideband antenna operation using several narrowband carriers with appropriately set phase shifts. In other words, only one beam in space is formed from a linear combination of several antenna beams having different carrier frequencies. This approach can enhance radar range resolution without needing time delays for the phase-based antenna controller. A version of the multi-beam system is experimentally demonstrated using rf devices. The concept can be extended to radar bands by using gigahertz band AODs, or using frequency up-conversion with microwave mixers. With current AOD technology, 32-64 channel AODs could be used in this wideband architecture.

6. REFERENCES

- [1] N. A. Riza, "Novel acousto-optic systems for spectrum analysis and phased array radar signal processing," chapter 6, Ph.D Thesis, Caltech, 1989.
- [2] N. A. Riza and D. Psaltis, "Acousto-optic signal processors for transmission and reception of phased array antenna signals," *Appl. Opt.*, vol.30, pp. , 1991.
- [3] N. A. Riza, "An acousto-optic phased array antenna beamformer with independent phase and carrier control using single sideband signals," *IEEE Photonics Tech. Lett.*, vol.4, No.2, pp.177-179, Feb., 1992.
- [4] N. A. Riza, "Acousto-optic architectures for multi-dimensional phased array antenna processing," in *Proc. SPIE Conf. Opt. Technol. Microwave Appl.*, vol.1476, pp. 144-156, 1991.
- [5] N. A. Riza, "An acousto-optic phased array antenna beamformer for multiple simultaneous beam generation," *IEEE Photonics Tech. Lett.*, vol.4, No.7, pp.807- 809, July, 1992.

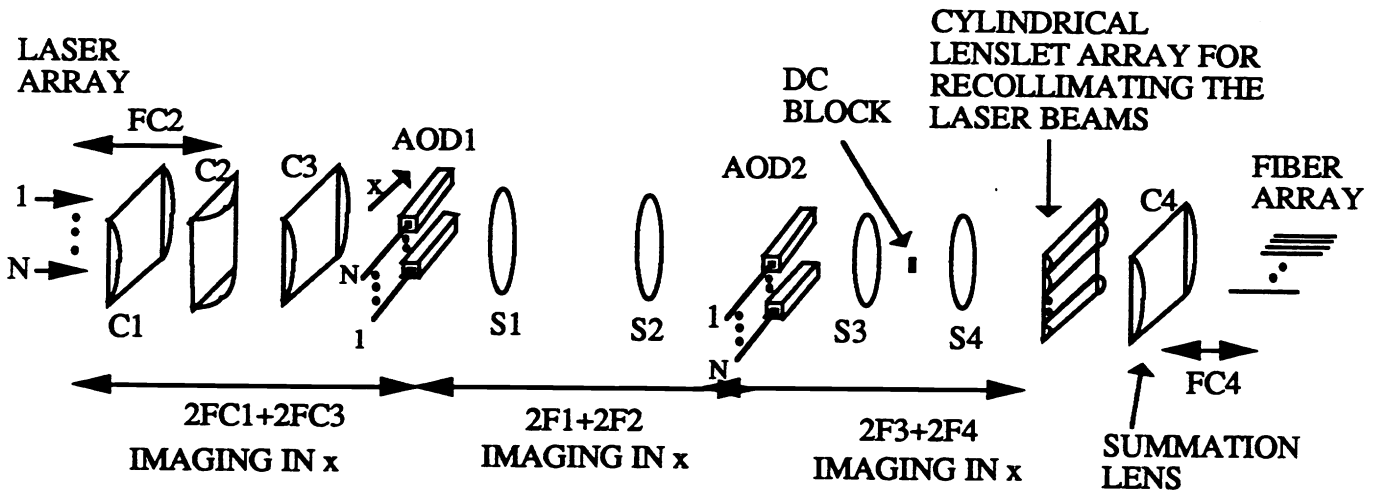


Fig.1 Basic architecture of the multiple simultaneous beamforming AO system.

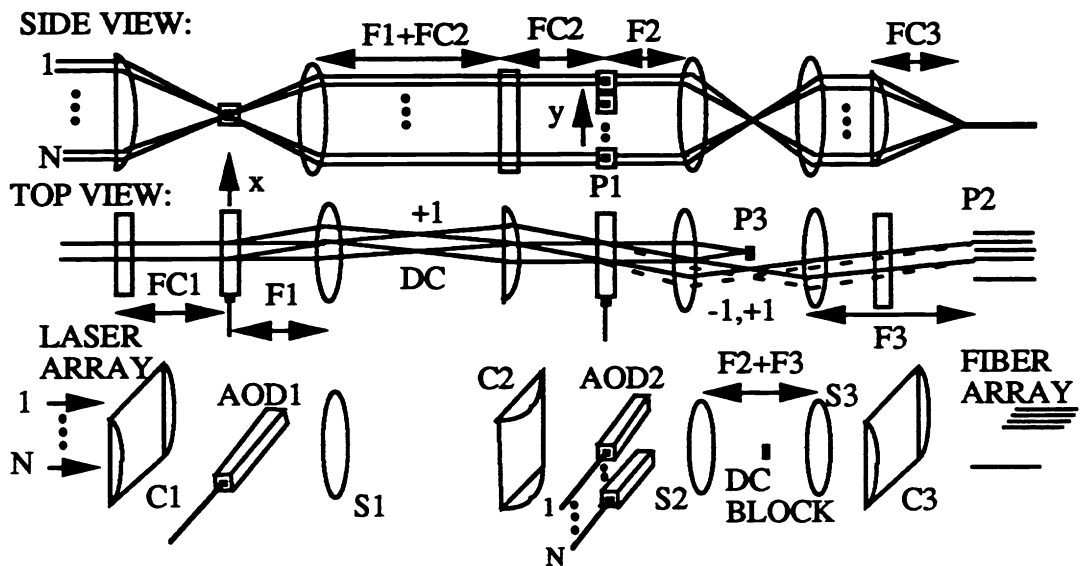


Fig.2 A version of the basic multiple simultaneous beamforming AO system architecture that is used for experimental concept demonstration.

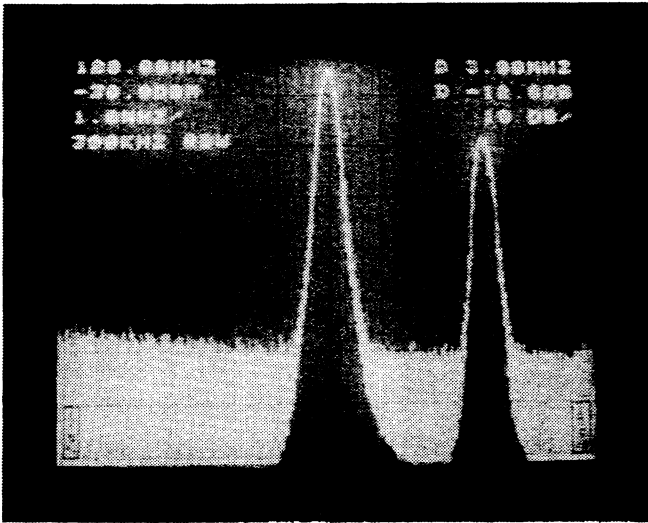


Fig.3 Spectrum analyzer trace showing the presence of two simultaneous carriers, one at 120 MHz (center one), and the other at 123 MHz, in the photo-current output of the AO system. Frequency scale: 1 MHz/div.

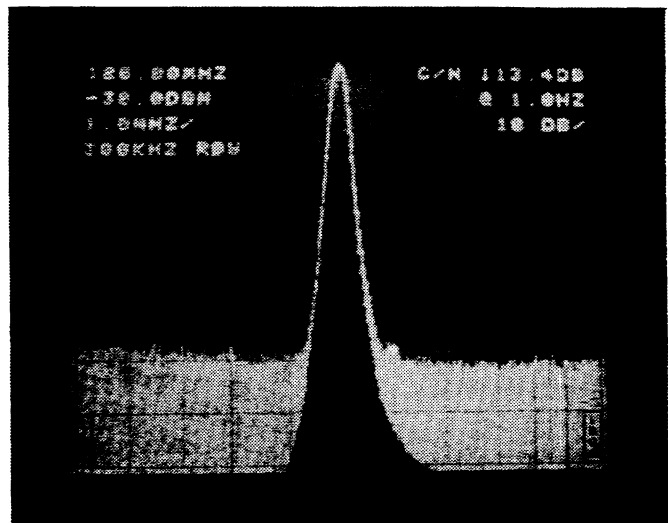
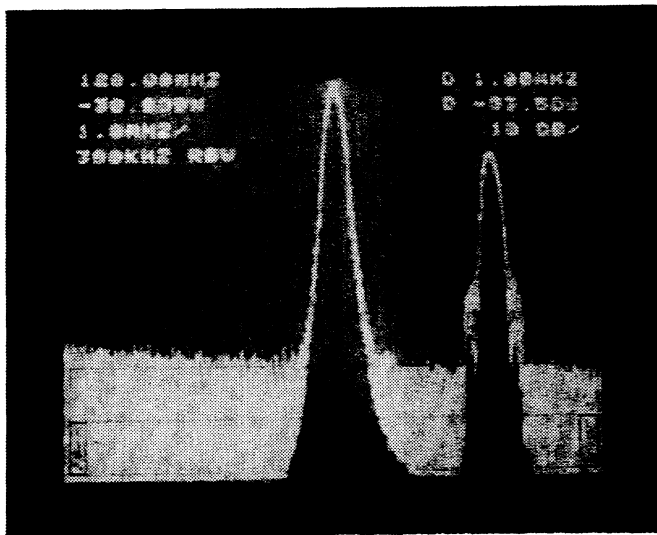
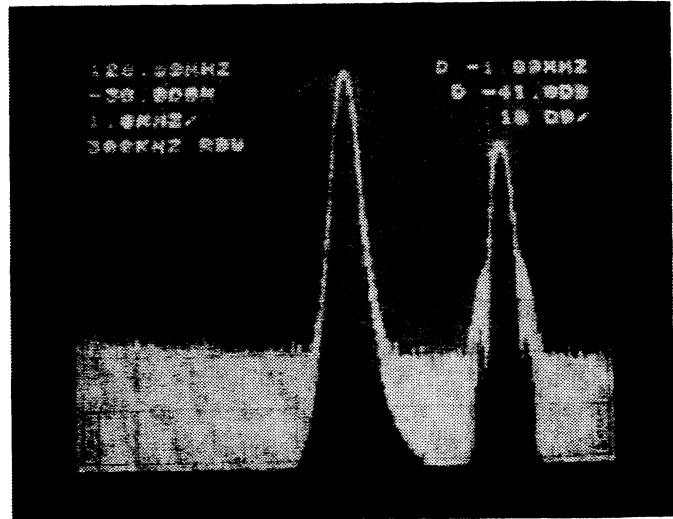


Fig.5 The carrier-to-noise ratio measured for the 120 MHz signal was 113.4 dB/Hz at 1 MHz.



(a)



(b)

Fig.4 The dynamic ranges measured for the 120 MHz and 123 MHz signals are (a) 53.5 dB at 1 MHz and (b) 41.8 dB at 1 MHz, respectively.

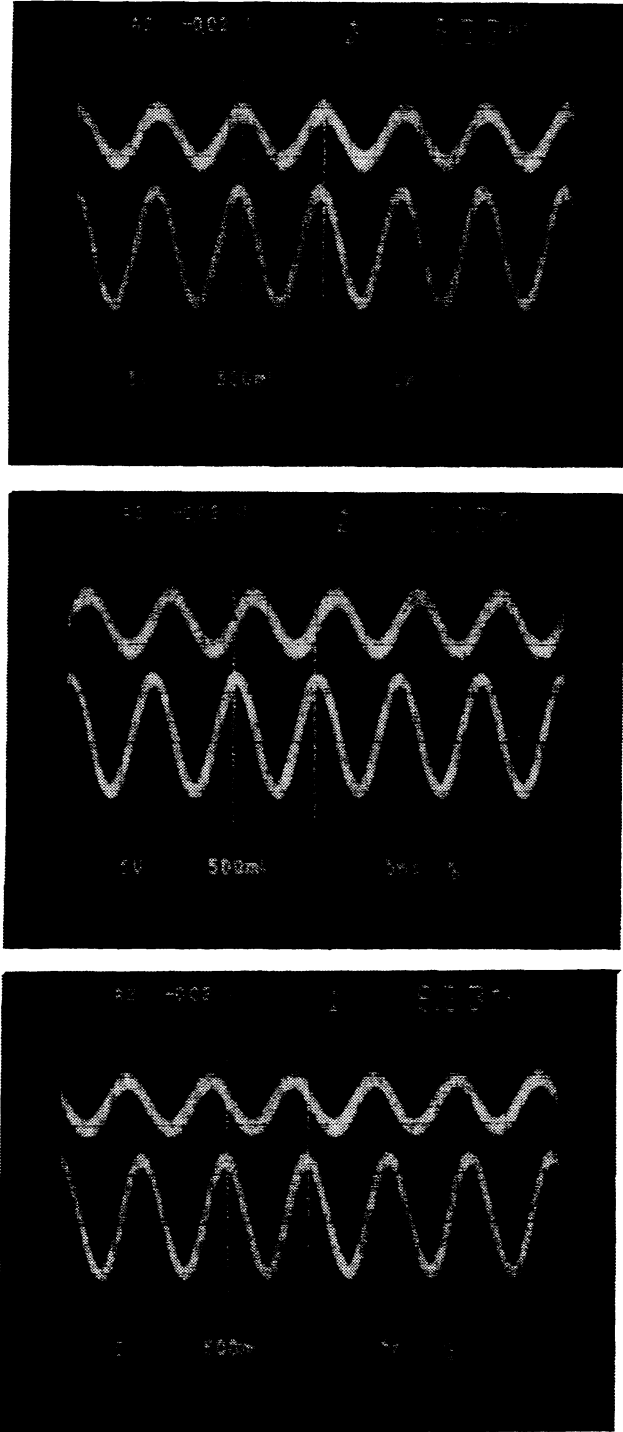


Fig.6 Oscilloscope traces showing $0-2\pi$ phase shifts of the rf signals generated by the photo-diode pair at the output plane of the processor. Here $2f_c=120$ MHz. Upper trace: 5V/div; lower trace: 500 mV/div; time scale: 5 nsec/div.

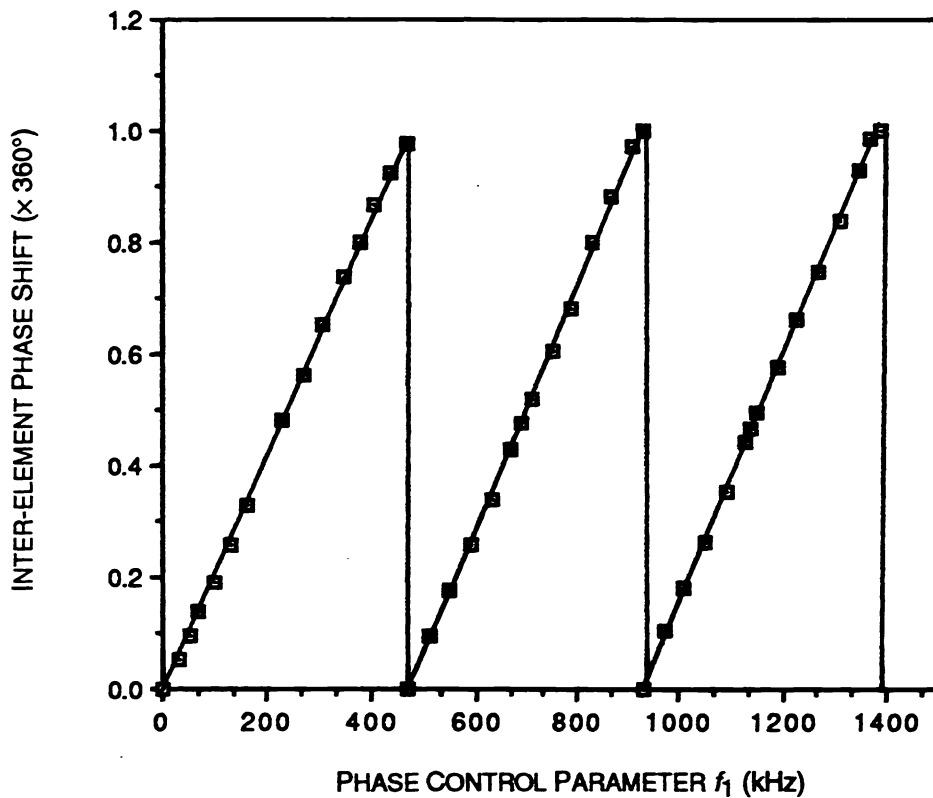


Fig.7 Experimental plot showing the change in relative phase ($0-2\pi$) for the rf signals from the photo-diode pair as the phase control parameter f_1 (KHz) is varied. Note the modulo- 2π nature of the phase sampling process, with a period $f_1=460$ KHz. For the experiment, $2f_c=120$ MHz.

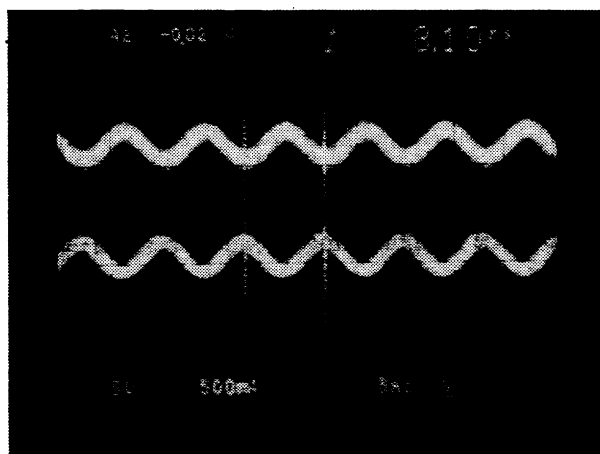
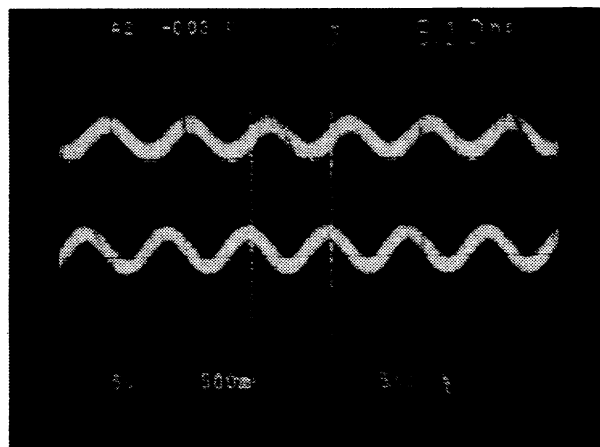
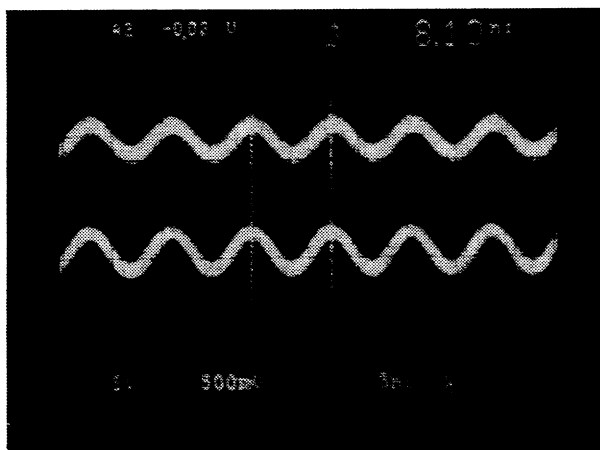


Fig.8 The $0-2\pi$ phase shift control for a 123.22 MHz + f_1 KHz carrier. Here $2f_c + 7f_1 = 120 \text{ MHz} + 7 \times 460 \text{ KHz} = 123.22 \text{ MHz}$.